Atmos. Chem. Phys. Discuss., 14, 1159–1190, 2014
www.atmos-chem-phys-discuss.net/14/1159/2014/
doi:10.5194/acpd-14-1159-2014
© Author(s) 2014. CC Attribution 3.0 License.

Atmospheric Chemistry and Physics
Discussions
Open Access

This discussion paper is/has been under review for the journal Atmospheric Chemistry and Physics (ACP). Please refer to the corresponding final paper in ACP if available.

Missing SO_2 oxidant in the coastal atmosphere? – Evidence from high resolution measurements of OH and atmospheric sulfur compounds

H. Berresheim[1], M. Adam[1], C. Monahan[1], C. O'Dowd[1], J. M. C. Plane[2], B. Bohn[3], and F. Rohrer[3]

[1]School of Physics & Centre for Climate and Air Pollution Studies, National University of Ireland Galway, Ireland
[2]School of Chemistry, University of Leeds, UK
[3]Institute for Energy and Climate Research (IEK-8: Troposphere), Research Center Jülich, Germany

Received: 13 December 2013 – Accepted: 28 December 2013 – Published: 15 January 2014

Correspondence to: F. Rohrer (f.rohrer@fz-juelich.de)

Published by Copernicus Publications on behalf of the European Geosciences Union.

Abstract

Diurnal and seasonal variations of gaseous sulfuric acid (H_2SO_4) and methane sulfonic acid (MSA) were measured in N.E. Atlantic air at the Mace Head atmospheric research station during the years 2010 and 2011. The measurements utilized selected ion/chemical ionization mass spectrometry (SI/CIMS) with a detection limit for both compounds of 4.3×10^4 cm^{-3} at 5 min signal integration. The H_2SO_4 and MSA gas-phase concentrations were analysed in conjunction with the condensational sink for both compounds derived from 3 nm–10 µm (diameter) aerosol size distributions. Accommodation coefficients of 1.0 for H_2SO_4 and 0.12 for MSA were assumed leading to estimated atmospheric lifetimes of the order of 7 min and 25 min, respectively. With the SI/CIMS instrument in OH measurement mode alternating between OH signal and background (non-OH) signal evidence was obtained for the presence of one or more unknown oxidants of SO_2 in addition to OH. Depending on the nature of the oxidant(s) their ambient concentration may be enhanced in the CIMS inlet system by additional production. The apparent unknown SO_2 oxidant was additionally confirmed by direct measurements of SO_2 in conjunction with calculated H_2SO_4 concentrations. The calculated concentrations were consistently lower than the measured concentrations by a factor 4.8 ± 3.4 when considering the oxidation of SO_2 by OH as the only source of H_2SO_4. Both the OH and the background signal were also observed to increase significantly during daytime aerosol nucleation events, independent of the ozone photolysis frequency, $J(O^1D)$, and were followed by peaks in both H_2SO_4 and MSA concentrations. This suggests a strong relation between the unknown oxidant(s), OH chemistry, and the atmospheric photo-oxidation of biogenic iodine compounds. As to the identity of the oxidant(s), we have been able to exclude ClO, BrO, IO, and OIO as possible candidates based on ab initio calculations. Stabilized Criegee intermediates (sCI) produced from ozonolysis of alkenes potentially contribute to the oxidation efficiency of the coastal and marine atmosphere. However, analysis of the CIMS background signal in context with recently published kinetic data currently suggests that larger Criegee

CC BY

intermediates produced from ozonolysis play no significant role for SO_2 oxidation in the marine atmosphere. The possibility of H_2SO_4 formation without SO_2 as precursor or from SO_2 oxidation by small sCI produced photolytically should be explored.

1 Introduction

It has been well established that homogeneous oxidation of tropospheric gases is generally dominated by reactions with the hydroxyl (OH) radical during daylight hours and – in regions with significant nitrogen oxide, NO_x, concentrations – with the nitrate (NO_3) radical in the absence of sunlight (Stone et al., 2012). Reactions of molecular oxygen, ozone, or peroxy radicals such as HO_2 and RO_2 (R = organic rest molecule) are comparatively slow, with few exceptions, such as $NO + HO_2$ which recycles OH (e.g., Atkinson et al., 2004). Heterogeneous oxidation (on the surface of aerosol particles and in cloud and fog droplets) is dominated either by reactions with dissolved ozone, hydrogen peroxide, or molecular oxygen, the latter pathway being catalyzed by transition metal ions (Harris et al., 2013; Berresheim and Jaeschke, 1986). However, recent studies have revived an interest in the formation and fate of atmospheric Criegee intermediates (RO_2 species produced from reactions of ozone with alkenes, Calvert et al., 2000) which to this day have eluded direct measurements in the atmosphere since Cox and Penkett (1971) first suggested their potentially important role. Field and laboratory measurements (Stone et al., 2014; Taatjes et al., 2013; Mauldin et al., 2012; Vereecken et al., 2012; Berndt et al., 2012; Welz et al., 2012) as well as theoretical studies (Boy et al., 2013) now suggest that the reactivity of these types of peroxy radicals towards compounds such as SO_2 may have been underestimated by at least two orders of magnitude. Therefore, in addition to OH – or possibly even rivalling OH chemistry – Criegee intermediates may, under certain conditions, be significant contributors to atmospheric sulfuric acid formation and the production of hygroscopic sulfate particles which can be activated as cloud condensation nuclei (CCN).

Selected ion – chemical ionization mass spectrometry (SI-CIMS) has been pioneered by Eisele and coworkers (Tanner and Eisele, 1995; Eisele and Tanner, 1993, 1991) for high time resolution measurements of OH, H_2SO_4, MSA(g) (gaseous methane sulfonic acid), and other compounds in the troposphere. A large number of field studies both on the ground as well as airborne have been successfully conducted using this technique and significantly improved our understanding of tropospheric chemistry (e.g., Stone et al., 2012; Huey, 2007; Heard and Pilling, 2003). In some of these studies it has already been conjectured that SI/CIMS may also provide information about the presence of atmospheric oxidants other than OH by analyzing the background signal recordings obtained in the OH measurement mode. Specifically, the identity of those "background X-oxidant(s)" was speculated to be Criegee intermediates because of their observed reactivity towards SO_2 in the measurement system (e.g., Berresheim et al., 2002).

In the present paper we have analyzed 2 yr of SI/CIMS measurements made at Mace Head, Ireland, for significant occurrences of such background signals indicating the presence of one or more unknown oxidants in coastal air which contribute to H_2SO_4 formation by oxidizing SO_2 (in addition to OH) during day- and nighttime. Furthermore, balance calculations of ambient H_2SO_4 levels using measured SO_2, OH, and aerosol particle concentrations have been compared with measured H_2SO_4 levels. This allowed us to approximate corresponding contributions to ambient H_2SO_4 levels from oxidation of SO_2 by oxidants other than OH and estimate their relative importance with respect to OH reactivity.

2 Experimental

A principle scheme of the Mace Head CIMS instrument and its operation is shown in Fig. 1. Similar to previously described systems (Berresheim et al., 2013, 2000; Mauldin et al., 2012, 1998) the aerodynamically shaped main air inlet extrudes retractably through the wall of the building, here towards the open ocean with a marine wind sector of 190–300°. In the following text, “marine sector” data includes only the subset of data consistent with the marine wind sector, NO levels < 50 pptv, and/or black carbon concentrations < 50 ng m^{-3}. From the main air flow (approximately 2.5 m^3 hr^{-1}) the central region is sampled at 12 slpm through a 1.9 cm diameter sample flow tube. Two pairs of oppositely arranged capillary stainless steel injectors (the front pair sitting upflow, the rear pair downflow at 5.2 cm distance from each other) protrude into the sample flow tube. Depending on the operational mode (OH signal measurement, OH background measurement, or H_2SO_4 and MSA(g) measurement) selected flows of SO_2, propane (C_3H_8), and N_2 (as make-up gas) are added through the injectors to the sample flow.

For measuring an OH signal isotopically heavy $^{34}SO_2$ (98.8 %, Eurisotop, Saint-Aubin, France) is introduced through the front injectors and mixed into the sample air flow resulting in a SO_2 mixing ratio of approximately 8 ppmv. At this setting, the OH lifetime (1/*e* definition) in the sample flow is 6 ms. The ambient OH concentration introduced into the CIMS system is completely converted to $H_2^{34}SO_4$ by its reaction with $^{34}SO_2$ within the available reaction time of $\tau_{\text{reac,OH}} = 78$ ms before reaching the rear injectors. Approximately 1 % of the resulting product, $H_2^{34}SO_4$, is converted via chemical ionization at atmospheric pressure by NO_3^- reactant ions into $H^{34}SO_4^-$ product ions which are then focussed and guided by electrical potentials (along with remaining NO_3^- ions) through a 80 µm aperture into the vacuum mass spectrometry region. The reactant ions are produced in a sheath flow of purified ambient air with added HNO_3 passing by a radioactive ^{241}Am alpha emitter (activity: 4.1 MBq; Eckert & Ziegler, Berlin, Germany). Detection of the $H^{34}SO_4^-$ signal at m/z 99 following quadrupole mass filtering yields the equivalent concentration of OH in ambient air. Applying the same method of ionization, ambient sulfuric acid, H_2SO_4, and methane sulfonic acid, CH_3SO_3H, in which sulfur occurs as ^{32}S at a fraction of 0.95 (Krouse and Grinenko, 1991) are detected at m/z 97 and m/z 95, respectively. Time resolution for measuring all three masses is typically 30 s. In general, measurement signals are integrated to 5 min with corresponding detection limits of $1.3 \times 10^5\,\mathrm{cm}^{-3}$ for OH and $4.3 \times 10^4\,\mathrm{cm}^{-3}$ for both H_2SO_4 and MSA(g), respectively (Berresheim et al., 2013; Mauldin et al., 1998). Further details including calibration procedures can be found in Berresheim et al. (2000).

Propane (99.95 %, Air Liquide, UK) is introduced into the sample flow through the rear injectors (establishing a mixing ratio of approximately 430 ppmv in the sample flow) to scavenge any OH which might be recycled from peroxy radicals via reaction with nitric oxide, NO. On average, nighttime OH measurements showed no major increase in the background signal compared to the OH signal suggesting any potential interference by trace contaminants in the propane to be negligible. Due to similar rate constants for SO_2 and propane with respect to their reaction with OH (both ca. $1 \times 10^{-12}\,\mathrm{cm}^3\,\mathrm{s}^{-1}$ at 298 K; Atkinson et al., 2004) any (recycled) OH molecules are scavenged by propane instead of SO_2 from this point, i.e., downflow from the rear injectors. Due to the very low NO mixing ratios in marine air at Mace Head (Berresheim et al., 2013) contributions to the measurement signal from the recycling of OH are expected to be negligible.

The background (BG) signal in the OH measurement mode is evaluated by switching the propane flow from the rear to the front injectors. This prevents formation of $H^{34}SO_4^-$ ions resulting from $^{34}SO_2 + OH$ reaction in the system. Theoretically, any background counts observed at m/z 99 under these conditions should only reflect the 4.2 % fraction of ^{34}S occurring in ambient H_2SO_4. If a significantly higher BG count is observed this might indicate the presence of a compound with stronger electron affinity than HNO_3 ending up as a product ion at m/z 99. However, experiments conducted without $^{34}SO_2$ in the system never showed any evidence for the existence of such a compound. Therefore, observations of significant BG signals (above the ambient 4.2 % $H^{34}SO_4^-$ signal) suggested the presence of one or more unknown oxidants converting $^{34}SO_2$ to $H_2^{34}SO_4$ in the CIMS system without appreciably reacting with propane. Indeed this interpretation was corroborated by stopping the SO_2 injection to the sample flow and observing a corresponding reduction in the m/z 99 BG signal. Furthermore, with SO_2 in the system, the propane flow through the front injector was successively increased from zero to the operational setting for measuring the BG signal. Before reaching this setting the signal was found to tail off to a background level corresponding to the complete removal of OH. Increasing the propane flow did not further alter the BG signal.

The total reaction time $\tau_{\mathrm{reac},X}$ available to this unknown oxidant "X" to react with SO_2 in the system forming H_2SO_4 is the time starting when a unit volume of the sample flow passes the position of the first injector pairs until it reaches the end of the atmospheric pressure ionization region, i.e., the 80 µm aperture (see Fig. 1). That time in our system corresponds to 0.45 s, or approximately half a second, which is about six times longer than $\tau_{\mathrm{reac,OH}}$. Therefore, the relative importance of X in comparison to the atmospheric oxidation efficiency of OH may have to be downscaled dependent on the properties of X and its potential formation and/or regeneration during the reaction time. This will be examined in detail in Sect. 3.4.

Photolysis frequencies of ozone, $J(O^1D)$, and of nitrogen dioxide, $J(NO_2)$, were measured since September 2010 on top of a 10 m tower next to the laboratory building. Both were exchanged with recalibrated systems on a semiannual basis. Details of the measurement principles and performance of the radiometers have been given by Bohn et al. (2008). SO_2 was measured in May–August 2011 with a Thermo Systems 43i instrument using a heated sample inlet teflon tubing (40 °C) to avoid SO_2 losses due to water condensate. Based on a cycle of 30 min signal and 30 min zero measurements (with an added active charcoal filter) we calculated a 2σ detection limit of 25 pptv for 1 h time integration.

3 Results and discussion

3.1 Seasonal cycles and atmospheric lifetimes of H_2SO_4 and MSA(g)

Figure 2 shows the mean seasonal cycle of the daily maximum H_2SO_4 concentration in the marine sector at Mace Head which typically occurred between 10–14 h local time, depending on cloud cover. In general, H_2SO_4 showed a clear diel variation closely correlated with the OH concentration (Fig. 3, top). The reason for this correlation was the

CC BY

relatively homogeneous mixing ratio of the major precursor, SO_2, in the marine atmosphere, as shown for a three months period in Fig. 4 (top), and the relatively short lifetime of H_2SO_4 caused by uptake onto aerosol surfaces. This so called condensational sink (CS) showed also low variability on most days (Fig. 4, bottom). The mean SO_2 mixing ratio in the open ocean sector was 160 (±50) pptv during these summer months. The average atmospheric lifetime of H_2SO_4 with respect to CS was estimated from SMPS and APS measurements using the approach of Fuchs and Sutugin (1971) and Pandis and Seinfeld (1998) to be on the order of 7 min assuming an accommodation coefficient of 1.0 (Kolb et al., 2010; Hanson, 2005; Boy et al., 2005), a diffusion coefficient for $H_2SO_4(2\,H_2O)$ of $0.075\,\mathrm{atm\,cm^2\,s^{-1}}$ at 75–85 % relative humidity (Hanson, 2005), a mean free path of 105 nm for $H_2SO_4(2\,H_2O)$ (corresponding to the Fuchs and Sutugin parameterization), and a hygroscopic growth factor of 1.7 (Bialek et al., 2012). Overall, we estimate that CS values can be uncertain by at least a factor of two, mainly due to the uncertainties in the count rates of the SMPS and APS instruments and of the hygroscopic growth factor.

At Mace Head we assume that the predominant source for H_2SO_4 in the marine atmosphere is ultimately biogenic, i.e., the emission and oxidation of dimethyl sulfide (DMS) by OH which yields – via further oxidation of intermediate compounds – the gaseous end products H_2SO_4, dimethyl sulfone ($CH_3SO_2CH_3$, $DMSO_2$), and methane sulfonic acid (CH_3SO_3H, MSA) (Berresheim et al., 1995, 1993a). As described in the previous section, the two acid compounds are detectable by SI/CIMS using the same instrumental setting as for the OH measurement. Corresponding seasonal cycles of aerosol MSA and non-sea salt sulfate, nss-SO_4, have been measured at Mace Head using high-resolution time-of-flight aerosol mass spectrometry (HR-TOF-MS). Both aerosol compounds as well as their concentration ratio show a clear seasonal maximum in summer (Ovadnevaite et al., 2013).

The mean seasonal cycle of peak MSA(g) mixing ratios recorded during the same daily time slot as for H_2SO_4 and summarized as monthly means is also shown in Fig. 2. Similar to H_2SO_4 and the aerosol sulfur compounds, the highest gas phase MSA(g) levels in the marine atmosphere were observed during the summer months which corroborates the biogenic origin of H_2SO_4 measured in this sector. Adopting a sticking coefficient of 0.12 for the aerosol scavenging of MSA(g) (De Bruyn et al., 1994) we obtained an average atmospheric lifetime of approximately half hour (25 min) for this compound. As for H_2SO_4 this is somewhat shorter than previously estimated from measurements off the north-western coast of the United States (Berresheim et al., 1993b), however, still within the same order of magnitude. Ammann et al. (2013) have questioned the earlier results obtained by De Bruyn et al. (1994) and Schweitzer et al. (1998) for the MSA(g) accommodation coefficient and suggested preferring a value close to one as reported in the most recent study by Hanson (2005). However, in our view, adopting a unity value would be in contradiction to common observations of a relatively slower decline of atmospheric MSA(g) levels in comparison to H_2SO_4 in late afternoon and evening hours which has been well documented in previous field studies (e.g., Eisele and Tanner, 1993) and in our present study. Furthermore, as shown already in a previous campaign at Mace Head (Berresheim et al., 2002), ambient MSA(g) levels typically increased with decreasing relative humidity, including at nighttime. Both observations support that the vapor pressure of MSA(g) is significantly higher compared to H_2SO_4 (e.g., Kreidenweis and Seinfeld, 1988).

3.2 H_2SO_4 mass balance and missing SO_2 oxidant in the marine atmosphere

From 2 May to 12 August 2011, an intensive campaign was conducted at Mace Head including measurements of SO_2. The results allowed the calculation of H_2SO_4 concentrations based on its production by SO_2 oxidation by OH and removal due to condensation on existing aerosol surface (CS, condensational sink rate):

$$[H_2SO_4]_{calc} = \frac{k_{OH}[SO_2][OH]}{CS} \quad (1)$$

Comparison with measured H_2SO_4 concentrations showed a significant underestimation using Eq. (1), bearing in mind the uncertainty in CS can be a factor of two. For

cc BY

all measurement days of the campaign, the mean ratio, i.e., $[H_2SO_4]_{meas}/[H_2SO_4]_{calc}$, was 4.8 (±3.4) during the midday periods of 10–14 UTC. This is considerably higher than the mean of 2.4 reported by Mauldin et al. (2012) for a boreal forest site in Finland. An example from 18 June 2011, is shown in Fig. 5, and Fig. 6 shows the overall mean of all measurements in the marine air mass sector. Both figures demonstrate the significant level of the recorded background signal. On average, the measured $[H_2SO_4]$ concentrations in the example of Fig. 5 were a factor of 7 higher than the values calculated by Eq. (1). Clearly, a major source of H_2SO_4 in addition to OH oxidation of SO_2 is missing in this calculation.

A similar discrepancy between measured and calculated H_2SO_4 values in the coastal atmosphere of Mace Head was reported previously by Berresheim et al. (2002). They speculated that the missing source might be DMS oxidation with partial production of SO_3 instead of SO_2 as intermediate, which then readily forms H_2SO_4 with water vapour (Lin and Chameides, 1993). This possibility would also agree with kinetic pathways hypothesized for the DMS + OH oxidation in which CH_3SO_2 and CH_3SO_3 are formed as intermediates, both of which decompose thermally to SO_2 and SO_3, respectively (Berresheim et al., 1995). Alternatively, it was suggested that oxidant(s) in addition to OH might play a significant role in this environment, e.g., stabilized Criegee intermediates (sCI) which recently have been re-evaluated with respect to their potential oxidation of atmospheric SO_2 by Welz et al. (2012) and Mauldin et al. (2012). Studies in an Antarctic coastal location with strong marine DMS emissions (Jefferson et al., 1998; Davis et al., 1998) reported similar inconsistencies between measured H_2SO_4 levels and SO_2 mixing ratios required to close the mass balance based on $SO_2 + OH$ as the only source, even when assuming a very low H_2SO_4 accommodation coefficient of 0.5. The nitrate radical, NO_3, is not expected to be of any importance for nighttime SO_2 oxidation in such remote locations including Mace Head, at least not in air from the marine sector (Berresheim et al., 2013).

3.3 Electronic structure calculations on halogen oxide reactions with SO_2

Other candidates might be halogen oxide radicals, however, to our knowledge respective rate constants are available in the literature only for the reactions of IO and ClO with SO_2 (e.g., kinetics.nist.gov/kinetics/), which are three and six orders of magnitude smaller compared to k_{SO_2+OH}, respectively. We have made ab initio transition state energy calculations for the reactions of SO_2 with ClO, BrO, IO, and OIO using quantum theory. The hybrid density functional/Hartree-Fock B3LYP method was employed from within the Gaussian 09 suite of programs (Frisch et al., 2009), combined with an appropriate basis set for I (Glukhovtsev et al., 1995) and the standard $6\text{–}311+g(2d,p)$ triple zeta basis sets for Br, Cl, O and S. Following geometry optimizations of the transition states for the reactions of ClO, BrO, IO and OIO with SO_2, and the determination of their corresponding vibrational frequencies and (harmonic) zero-point energies, energies relative to the reactants were obtained. In the case of BrO and ClO + SO_2, more accurate transition state energies were computed at the CBS-QB3 level (Montgomery et al., 2000). At this level of theory, the expected uncertainty in the calculated transition state energies should be better than 0.07 eV (Foresman and Frisch, 1996). Spin-orbit effects were ignored since these are present both in the reactant halogen oxide and the transition state. Figure 7 illustrates the transition state geometries for ClO, BrO, IO and OIO + SO_2.

Transition state theory (TST) calculations were then carried out using the calculated molecular parameters in Table 1. Although the reaction between IO and SO_2 has a small barrier (7.3 kJ mol^{-1}), the reaction has quite a tight transition state and the TST calculation yields $k(200\text{–}400\,\mathrm{K}) = 4.3\times10^{-14}\exp(-1150/T)\,\mathrm{cm^3\,s^{-1}}$. The resulting value of $k(343\,\mathrm{K}) = 1.6\times10^{-15}\,\mathrm{cm^3\,s^{-1}}$ is consistent with an experimental upper limit of $6\times10^{-15}\,\mathrm{cm^3\,s^{-1}}$ determined at that temperature by Larin et al. (1998). At a marine boundary layer temperature of 293 K, the rate coefficient is only $8.5\times10^{-16}\,\mathrm{cm^3\,s^{-1}}$. This reaction would have to compete with OH + SO_2, which has a rate coefficient of $k = 9\times10^{-13}\,\mathrm{cm^3\,s^{-1}}$. Although [IO] can be around 30 times larger than [OH] at midday at Mace Head, the ratio of rate constants is 1/1050, so the OH reaction is about 35 times faster.

During nighttime at Mace Head, OIO builds up to a mixing ratio of a few parts per trillion (Saiz-Lopez and Plane, 2004). However, the very large barrier for the OIO + SO_2 reaction ($50.1\,kJ\,mol^{-1}$) means that this reaction is negligibly slow: $k(200–400\,K) = 6.4 \times 10^{-13} \exp(-6400/T)\,cm^3\,s^{-1}$, and $k(293\,K) = 2.2 \times 10^{-22}\,cm^3\,s^{-1}$.

BrO has been observed at a mixing ratio of several parts per trillion during the day at Mace Head (Saiz-Lopez et al., 2004). However, the reaction BrO + SO_2 also has a significant barrier ($20.4\,kJ\,mol^{-1}$), and so the reaction is much too slow in the MBL: $k(200–400\,K) = 5.8 \times 10^{-14} \exp(-2700/T)\,cm^3\,s^{-1}$, and $k(293\,K) = 5.6 \times 10^{-18}\,cm^3\,s^{-1}$. Finally, the TST calculation for ClO + SO_2, which also has a significant barrier ($24.1\,kJ\,mol^{-1}$), yields $k = 5.2 \times 10^{-14} \exp(-3100/T)\,cm^3\,s^{-1}$. The theoretical rate coefficient at 298 K is therefore $1.5 \times 10^{-18}\,cm^3\,s^{-1}$, which is in accord with an experimental upper limit of $4 \times 10^{-18}\,cm^3\,s^{-1}$ at this temperature (DeMore et al., 1997). In summary we conclude that none of the halogen oxides considered here react with SO_2 fast enough in ambient air to be likely candidates for the missing SO_2 oxidant(s).

3.4 Could *X* be a Criegee radical produced from ozonolysis?

Ignoring the possibility raised by Lin and Chameides (1992) of SO_3 being a major intermediate of DMS + OH oxidation, only the oxidation of SO_2 by sCI remains to be investigated based on current knowledge. If "*X*" is indeed a Criegee intermediate produced from ozonolysis of alkenes and reacting with SO_2 in the atmosphere and in the CIMS inlet system to produce additional H_2SO_4, we can estimate its relative contribution compared to the SO_2 + OH reaction as follows.

As already pointed out in the experimental section we have to account for additional formation of $[sCI]_{cims}$ from alkene + O_3 reactions over the total available residence time of 0.45 s in the atmospheric pressure reaction and ionization region of the CIMS instrument (see Fig. 1). By continuous reaction with SO_2 and ionization of the resulting

$H_2^{34}SO_4$ molecules over the corresponding distance (32 cm) this leads to an accumulation of the $H^{34}SO_4^-$ background signal at m/z 99 assuming the sCI + SO_2 oxidation to be instantaneous at the high SO_2 concentration in the CIMS reactor tube. The enhancement factor EF relative to the ambient air sCI concentration, $[\mathrm{sCI}]_{\mathrm{amb}}$, is

$$\mathrm{EF}_{H_2^{34}SO_4} = \frac{[\mathrm{sCI}]_{\mathrm{amb}} + \int_0^{t_{\mathrm{res}}} \mathrm{Prod(sCI)} \cdot \mathrm{d}t}{[\mathrm{sCI}]_{\mathrm{amb}}} = 1 + \frac{t_{\mathrm{res}}}{\tau_{\mathrm{sCI,amb}}} \qquad (2)$$

This result is the consequence of the fact that both types of sCI, namely sCI produced in ambient conditions ($\mathrm{sCI}_{\mathrm{amb}} = \mathrm{Prod(sCI)} \cdot \tau_{\mathrm{sCI,amb}}$) and sCI produced inside the CIMS inlet are immediately converted to $H_2^{34}SO_4$ by added $^{34}SO_2$ in the CIMS inlet system. Assuming a lifetime with respect to unimolecular decomposition of 0.2 s for sCI compounds resulting from ozonolysis of the monoterpenes α-pinene and limonene (Mauldin et al., supplement, 2012) and the dominant ambient reaction of sCI with water ($k_{H_2O+sCI} = 1.4 \times 10^{-17}\,\mathrm{cm^3\,s^{-1}}$ (MCM 3.2 http://mcm.leeds.ac.uk/MCM/; Saunders et al., 2003; Jenkin et al., 2003), $[H_2O] = 3.1 \times 10^{17}\,\mathrm{cm^{-3}}$ representing Mace Head conditions of T = 14 °C, 75 % relative humidity) the ambient lifetime of such stabilized Criegee intermediates is estimated to be 0.1 s. As already mentioned, approximately 1 % of the H_2SO_4 is ionized in the CIMS ionization region. Therefore, the production of sCI in this region indeed yields $H_2^{34}SO_4$ via reaction with $^{34}SO_2$, of which, however, only 0.5 % is ionized, on average, as this process acts linearly. Consequently, we have to modify Eq. (2) to take into account the reduced ionization probability for H_2SO_4 produced in the ionization region:

$$\mathrm{EF}_{H^{34}SO_4^-} = 1 + \frac{t_{\mathrm{reac}}}{\tau_{\mathrm{sCI,amb}}} + 0.5 \cdot \frac{t_{\mathrm{ion}}}{\tau_{\mathrm{sCI,amb}}} \qquad (3)$$

with $t_{\mathrm{res}} = 450\,\mathrm{ms}$, $t_{\mathrm{reac}} = 115\,\mathrm{ms}$, $t_{\mathrm{ion}} = 335\,\mathrm{ms}$, $\tau_{\mathrm{sCI,amb}}^{-1} = 1/0.2\,\mathrm{s} + 4.3\,\mathrm{s^{-1}} = 9.3\,\mathrm{s^{-1}}$. This formalism is identical to that derived for a similar instrument by Berndt et al. (2012)

(chemical ionization time-of-flight mass spectrometer with atmospheric pressure inlet; CI-APi-TOF-MS). Thus, from Eq. (3) it follows that $^{34}SO_2$ oxidation by sCI contributes a background signal which represents an enhancement of the ambient sCI concentration by a factor EF = 3.6. Therefore, if X is indeed a sCI compound (of the kind considered here), the measurement signal resulting from sCI would have to be weighted by 1 : 3.6 with respect to the OH signal to obtain the corresponding ambient air concentration [sCI]. To compare both compounds with respect to their oxidation efficiency towards SO_2, the corresponding rate constants must be factored in as well, i.e., $k_{sCI+SO_2}/k_{OH+SO_2} = 6 \times 10^{-13}\,cm^3\,s^{-1}/9 \times 10^{-13}\,cm^3\,s^{-1} = 0.67$, with k_{OH+SO_2} (298 K) = $9 \times 10^{-13}\,cm^3\,s^{-1}$ taken from Atkinson et al. (2004) and k_{sCI+SO_2} adopted for the (monoterpene + SO_2) reaction as reported by Mauldin et al. (2012). This means that the oxidation efficiency of those sCI compounds would be only on the order of 1 : 5.4, i.e., 20 % compared to that of OH with respect to SO_2 oxidation, assuming that the CIMS background signal is equal to the OH signal as observed on average in the ambient air measurements at Mace Head (see Fig. 6).

These calculations depend strongly on the kinetic parameters for the corresponding sCI reactions. In this work we have adopted rate constants published by Mauldin et al. (2012) and Berndt et al. (2012) for stabilized Criegee intermediates produced from ozonolysis of monoterpenes. However, other studies of smaller Criegee intermediates with low internal energies (CH_2OO by Stone et al. (2014) and Welz et al. (2012); CH_3CHOO by Taatjes et al., 2013a) suggest much faster reactions of these CI species with both SO_2 and H_2O, respectively. For a sensitivity test we take the parameters from Taatjes el al. (2013a), ($k(CI+SO_2) = 6.7 \times 10^{-11}$ and $2.4 \times 10^{-11}\,cm^3\,s^{-1}$, $k(CI+H_2O) = 1 \times 10^{-14}$ and an upper limit of $4 \times 10^{-15}\,cm^3\,s^{-1}$ for the anti and syn conformers of CH_3CHOO, respectively) and neglect the fact, that for the conditions in the CIMS inlet only 80 % of these CI would react with the added $^{34}SO_2$. We also neglect their unimolecular decomposition whose rate constant is given as an upper limit of 250 s^{-1} by Taatjes et al. (2013a), since this process would make only a small contribution to our estimates. We find that the oxidation efficiency of such CIs – if formed via ozonolysis – compared to OH would be approximately 1 : 11.8 for anti and 1 : 13.2 for syn conformers of CH_3CHOO compared to our earlier estimate of 1 : 5.4, again based on the condition of equal CIMS background and OH signal counts. The relatively small difference between these estimates is a consequence of the fact that both reaction parameters (for $CI + SO_2$ and $CI + H_2O$) are faster in this second estimate. The effect of a faster reaction of CI with SO_2 is almost exactly cancelled out by the faster reactions with H_2O.

For these reasons, if the oxidant(s) *X* would be such types of stabilized Criegee intermediates, the combined oxidation efficiency of both compounds is estimated to account for a factor of approximately 1.2, increasing the calculated H_2SO_4 concentration based on the $SO_2 + OH$ source alone by only 10–20 %. This is still a major shortfall with respect to the average factor of 4.8 required to match the observed ambient air H_2SO_4 concentration. Assuming a (rather unlikely) H_2SO_4 accommodation coefficient as low as 0.5 would reduce this discrepancy by only 30 %. As discussed earlier, we assume that much of the uncertainty remains with the calculation of the condensational sink. However, as yet unknown interferences in the CIMS background signal measurements cannot be entirely ruled out. It appears particularly puzzling that the BG signal frequently tracks the OH signal suggesting that *X* has similar sources and sinks as OH (Fig. 6). Good candidates for the origin of the CIMS background signal are stabilized Criegee intermediates or iodine oxide (see discussion below). The consequence for the ambient H_2SO_4 budget is more complex. Either different Criegee intermediates than those studied so far or an entirely different kind of oxidant for SO_2 or a production process converting a sulfur compound other than SO_2 might be still missing in our present account of the H_2SO_4 concentration in the coastal marine atmosphere.

Recently, Taatjes et al. (2013b) suggested that CH_2OO might be an important intermediate in marine air resulting from both ozonolysis of alkenes and photolysis of CH_2I_2. Studies by Stone et al. (2014) and Welz et al. (2012) point towards a significant role of this Criegee intermediate for atmospheric SO_2 oxidation. Figure 8 shows an example of several observations we made in relation to coastal aerosol nucleation events during which both H_2SO_4 and MSA(g) concentrations increased significantly in conjunction with a major increase in the background signal counts for the X-oxidant(s). A recent successful H_2SO_4 intercomparison experiment at Mace Head (M. Sipilä and S. Richters, personal communication, 2013) between the CIMS instrument and a CI-APi-TOF-MS instrument has confirmed that the CIMS indeed measures only the concentration of gaseous "free" (monomeric) H_2SO_4 during nucleation events. With the rapid transition from monomers to multimer clusters in which H_2SO_4 becomes tied up (confined) and not broken down anymore to the HSO_4^- core ions in the CIMS collision dissociation chamber (Fig. 1) a net decrease in ambient H_2SO_4 concentrations may therefore be expected. However, as shown in the nucleation event in Fig. 8, (monomer) H_2SO_4 levels even increased after a certain lag time following the onset of the event. We interpret our observations as strong formation of X-oxidant(s) and OH (perhaps via thermal decomposition of sCI; Berndt et al. (2012), Kroll et al., 2001) followed by rapid oxidation of DMS and SO_2 to form the products H_2SO_4 and MSA(g). A second, albeit less intensive event was registered on the same day during the evening low tide period ending near sunset (21:30 UTC). Even during this smaller event some increase in OH and X-oxidant levels could be observed. Such coastal nucleation events have previously been shown to be induced by photolysis and photo-oxidation of marine iodine compounds emitted mainly from exposed seaweed during low tide (O'Dowd et al., 2002). Considering again the $IO + SO_2$ reaction and adopting a rate constant of $k(IO + SO_2) = 8.9 \times 10^{-16}\,cm^3\,s^{-1}$ (Sect. 3.3), we calculate that approximately 8 % of atmospheric IO is converting $^{34}SO_2$ to $H_2^{34}SO_4$ in the CIMS inlet system, based on a $^{34}SO_2$ mixing ratio of 8 ppmv and a total IO residence time of 0.45 s. Also, it is assumed that IO does not react with propane. Based on Eq. (3) the corresponding yield for $H^{34}SO_4^-$ would be reduced from 8 % to 5 %. With this estimate an upper limit for the atmospheric IO mixing ratio can be derived from the corresponding CIMS background signal. We estimate ambient IO levels to be, on average, less than 1.3 pptv at noon time (Fig. 6) and less than 5 pptv at the maximum of the nucleation event shown in Fig. 8. This is consistent with previous measurements of IO at Mace Head which showed max-

cc BY

imum levels up to 5 pptv (Saiz-Lopez et al., 2006; Alicke et al., 1999). Future studies are required to systematically characterize remaining uncertainties in the CIMS and CS measurements and to verify a possible link between the unknown oxidant(s) and the iodine cycle in the marine atmosphere.

4 Conclusions

We observed a persistent but relatively low H_2SO_4 background concentration at nighttime (on the order of a few $10^5\,cm^{-3}$) with OH below the detection limit. Also, on some occasions short spikes were observed at nighttime in the background signal during low tide which might suggest short-term emissions of reactive hydrocarbons capable of forming sCI compounds and OH in reactions with ozone. We assume that such processes also happen during daytime but are superimposed by the formation of another major oxidant which shows a similar diurnal pattern like OH. Whether this oxidant might be a Criegee radical with its production mainly determined by strong light-induced emissions of marine hydrocarbon species and/or atmospheric photolysis of iodine species remains an open question. However, we consider it unlikely that α-pinene or limonene are present at significant levels in the marine atmosphere. For this reason and also based on the currently available kinetic data for the SO_2 oxidation by sCI compounds resulting from these monoterpenes we conclude that at least those specific sCI radicals are unimportant in comparison with the $SO_2 + OH$ oxidation in the marine atmosphere. In the present work we have shown that the OH background signal measured with the CIMS instrument provides evidence for the presence of one or more unknown oxidants for atmospheric SO_2 in addition to OH. However, as this oxidant X does not significantly react with propane in the CIMS system, the corresponding X-signal must be corrected to account for additional production inside the CIMS inlet system before evaluating its oxidation efficiency towards SO_2 in ambient air. However, it appears that Mauldin et al. (2012) have not considered this correction which reduces the proposed oxidation efficiency for SO_2 of stabilized Criegee intermediates from α-pinene or limonene in forested environments as well.

Acknowledgements. Financial support for this work was provided by Science Foundation Ireland (grant 09/RFP/GEO2176), EPA Ireland (grant 2007-INF-12-S5), Higher Education Authority Programme for Research in Third Level Institutes – Cycle 4, European Commission Framework programme projects EUCAARI, (036833-2), ACTRIS (262254), and EUSAAR.

References

Alicke, B., Hebestreit, K., Stutz, J., and Platt, U.: Iodine oxide in the marine boundary layer, Nature, 397, 572–573, 1999.

Ammann, M., Cox, R. A., Crowley, J. N., Jenkin, M. E., Mellouki, A., Rossi, M. J., Troe, J., and Wallington, T. J.: Evaluated kinetic and photochemical data for atmospheric chemistry: Volume VI – heterogeneous reactions with liquid substrates, Atmos. Chem. Phys., 13, 8045–8228, doi:10.5194/acp-13-8045-2013, 2013.

Atkinson, R., Baulch, D. L., Cox, R. A., Crowley, J. N., Hampson, R. F., Hynes, R. G., Jenkin, M. E., Rossi, M. J., and Troe, J.: Evaluated kinetic and photochemical data for atmospheric chemistry: Volume I – gas phase reactions of O_x, HO_x, NO_x and SO_x species, Atmos. Chem. Phys., 4, 1461–1738, doi:10.5194/acp-4-1461-2004, 2004.

Berndt, T., Jokinen, T., Mauldin III, R. L., Petäjä, T., Herrmann, H., Junninen, H., Paasonen, P., Worsnop, D. R., and Sipilä, M.: Gas-phase ozonolysis of selected olefins: the yield of stabilized Criegee intermediates and the reactivity toward SO_2, J. Phys. Chem. Lett., 3, 2892–2896 and supplement, 2012.

Berresheim, H. and Jaeschke, W.: Study of metal aerosol systems as a sink for atmospheric SO_2, J. Atmos. Chem., 4, 311–334, 1986.

Berresheim, H., Eisele, F. L., and Tanner, D. J.: Field studies of atmospheric DMS chemistry using selected ion chemical ionization mass spectrometry, in: Dimethylsulfide: Oceans, Atmosphere and Climate, edited by: Restelli, G. and Angeletti, G., Kluwer Academic Publishers, Dordrecht, 239–242, 1993a.

Berresheim, H., Eisele, F. L., Tanner, D. J., Covert, D. S., McInnes, L., and Ramsey-Bell, D. C.: Atmospheric sulfur chemistry and cloud condensation nuclei (CCN) concentrations over the northeastern Pacific coast, J. Geophys. Res., 98, 12701–12711, 1993b.

Berresheim, H., Wine, P. H., and Davis, D. D.: Sulfur in the atmosphere, in: Composition, Chemistry, and Climate of the Atmosphere, edited by: Singh, H. B., Van Nostrand Reinhold, New York, 251–307, 1995.

Berresheim, H., Elste, T., Plass-Dülmer, C., Eisele, F. L., and Tanner, D. J.: Chemical ionization mass spectrometer for long-term measurements of atmospheric OH and H_2SO_4, Int. J. Mass Spectrom., 202, 91–109, 2000.

Berresheim, H., Elste, T., Tremmel, H. G., Allen, A. G., Hansson, H.-C., Rosman, K., Dal-Maso, M., Mäkelä, J. M., Kulmala, M. and O'Dowd, C. D.: Gas-aerosol relationships of H_2SO_4, MSA, and OH: observations in the coastal marine boundary layer at Mace Head, Ireland, J. Geophys. Res., 107, 8100, doi:10.1029/2000JD000229, 2002.

Berresheim, H., McGrath, J., Adam, M., Mauldin III, R. L., Bohn, B., and Rohrer, F.: Seasonal Measurements of OH, NO_x, and $J(O^1D)$ at Mace Head, Ireland, Geophys. Res. Lett., 40, 1659–1663, 2013.

Bialek, J., Dall'Osto, M., Monahan, C., Beddows, D., and O'Dowd, C.: On the contribution of organics to the North East Atlantic aerosol number concentration, Environ. Res. Lett., 7, 044013, doi:10.1088/1748-9326/7/4/044013, 2012.

Bohn, B., Corlett, G. K., Gillmann, M., Sanghavi, S., Stange, G., Tensing, E., Vrekoussis, M., Bloss, W. J., Clapp, L. J., Kortner, M., Dorn, H.-P., Monks, P. S., Platt, U., Plass-Dülmer, C., Mihalopoulos, N., Heard, D. E., Clemitshaw, K. C., Meixner, F. X., Prevot, A. S. H., and Schmitt, R.: Photolysis frequency measurement techniques: results of a comparison within the ACCENT project, Atmos. Chem. Phys., 8, 5373–5391, doi:10.5194/acp-8-5373-2008, 2008.

Boy, M., Mogensen, D., Smolander, S., Zhou, L., Nieminen, T., Paasonen, P., Plass-Dülmer, C., Sipilä, M., Petäjä, T., Mauldin, L., Berresheim, H., and Kulmala, M.: Oxidation of SO_2 by stabilized Criegee intermediate (sCI) radicals as a crucial source for atmospheric sulfuric acid concentrations, Atmos. Chem. Phys., 13, 3865–3879, doi:10.5194/acp-13-3865-2013, 2013.

Boy, M., Kulmala, M., Ruuskanen, T. M., Pihlatie, M., Reissell, A., Aalto, P. P., Keronen, P., Dal Maso, M., Hellen, H., Hakola, H., Jansson, R., Hanke, M., and Arnold, F.: Sulphuric acid closure and contribution to nucleation mode particle growth, Atmos. Chem. Phys., 5, 863–878, doi:10.5194/acp-5-863-2005, 2005.

cc BY

Calvert, J. G., Atkinson, R., Kerr, J. A., Madronich, S., Moortgat, G. K., Wallington, T. J., and Yarwood, G.: The Mechanisms of Atmospheric Oxidation of Alkenes, Oxford University Press, New York, ISBN 0-19-513177-0, 2000.

Cox, R. A. and Penkett, S. A.: Oxidation of atmospheric SO_2 by products of the ozone–olefin reaction, Nature, 230, 321–322, 1971.

Davis, D., Chen, G., Kasibhatla, P., Jefferson, A., Tanner, D., Eisele, F., Lenschow, D., Neff, W., and Berresheim, H.: DMS oxidation in the Antarctic marine boundary layer: comparison of model simulations and field observations of DMS, DMSO, $DMSO_2$, H_2SO_4(g), MSA(g), and MSA(p), J. Geophys. Res., 103, 1657–1678, 1998.

De Bruyn, W. J., Shorter, J. A., Davidovits, P., Worsnop, D. R., Zahniser, M. S., and Kolb, C. E.: Uptake of gas phase sulfur species methanesulfonic acid, dimethylsulfoxide, and dimethyl sulfone by aqueous surfaces, J. Geophys. Res., 99, 16927–16932, doi:10.1029/94JD00684, 1994.

DeMore, W. B., Sander, S. P., Golden, D. M., Hampson, R. F., Kurylo, M. J., Howard, C. J., Ravishankara, A. R., Kolb, C. E., and Molina, M. J.: Chemical kinetics and photochemical data for use in stratospheric modeling, Evaluation number 12, JPL Publication, 97–4, 1–266, 1997.

Eisele, F. L. and Tanner, D. J.: Ion-assisted tropospheric OH measurements, J. Geophys. Res., 96, 9295–9308, 1991.

Eisele, F. and Tanner, D.: Measurement of the gas phase concentration of H_2SO_4 and methane sulfonic acid and estimates of H_2SO_4 production and loss in the atmosphere, J. Geophys. Res,. 98, 9001–9010, 1993.

Foresman, J. B. and Frisch, A.: Exploring Chemistry with Electronic Structure Methods, Gaussian, Inc., Pittsburgh, 1996.

Frisch, M. J. , Trucks, G. W., Schlegel, H. B., Scuseria, G. E., Robb, M. A., Cheeseman, J. R., Scalmani, G., Barone, V., Mennucci, B., Petersson, G. A., Nakatsuji, H., Caricato, M., Li, X., Hratchian, H. P., Izmaylov, A. F., Bloino, J., Zheng, G., Sonnenberg, J. L., Hada, M., Ehara, M., Toyota, K., Fukuda, R., Hasegawa, J., Ishida, M., Nakajima, T., Honda, Y., Kitao, O., Nakai, H., Vreven, T., Montgomery, J. A., Peralta, J. E., Ogliaro, F., Bearpark, M., Heyd, J. J., Brothers, E., Kudin, K. N., Staroverov, V. N., Kobayashi, R., Normand, J., Raghavachari, K., Rendell, A., Burant, J. C., Iyengar, S. S., Tomasi, J., Cossi, M., Rega, N., Millam, J. M., Klene, M., Knox, J. E., Cross, J. B., Bakken, V., Adamo, C., Jaramillo, J., Gomperts, R., Stratmann, R. E., Yazyev, O., Austin, A. J., Cammi, R., Pomelli, C., Ochterski, J. W.,

cc BY

Martin, R. L., Morokuma, K., Zakrzewski, V. G., Voth, G. A., Salvador, P., Dannenberg, J. J., Dapprich, S., Daniels, A. D., Farkas, O., Foresman, J. B., Ortiz, J. V., Cioslowski, J., and Fox, D. J.: Gaussian 09, Revision A.1. Gaussian, Inc., Wallingford, CT, USA, 2009.

Fuchs, N. and Sutugin, A.: Highly dispersed aerosol, in: Topics in Current Aerosol Research, edited by: Hidy, G. and Brock, J., Pergamon, New York, 1–60, 1971.

Glukhovtsev, M. N., Pross, A., McGrath, M. P., and Radom, L.: Extension of Gaussian-2 (G2) theory to bromine- and iodine-containing molecules: use of effective core potentials, J. Chem. Phys., 103, 1878–1885, 1995.

Hanson, D. R.: Mass accommodation of H_2SO_4 and CH_3SO_3H on water-sulfuric acid solutions from 6 % to 97 % rH, J. Phys. Chem. A, 109, 6919–6927, 2005.

Harris, E., Sinha, B., van Pinxteren, D., Tilgner, A., Fomba, K. W., Schneider, J., Roth, A., Gnauk, T., Fahlbusch, B., Mertes, S., Lee, T., Collett, J., Foley, S., Borrmann, S., Hoppe, P., and Herrmann, H.: Enhanced role of transition metal ion catalysis during in-cloud oxidation of SO_2, Science, 340, 727–730, 2013.

Heard, D. E. and Pilling, M. J.: Measurement of OH and HO_2 in the troposphere, Chem. Rev., 103, 5163–5198, 2003.

Huey, G. L.: Measurement of trace atmospheric species by chemical ionization mass spectrometry: speciation of reactive nitrogen and future directions, Mass Spectrom. Rev., 26, 166–184, 2007.

Jefferson, A., Tanner, D. J., Eisele, F. L., and Berresheim, H.: Sources and sinks of H_2SO_4 in the remote Antarctic marine boundary layer, J. Geophys. Res., 103, 1639–1645, 1998.

Jenkin, M. E., Saunders, S. M., Wagner, V., and Pilling, M. J.: Protocol for the development of the Master Chemical Mechanism, MCM v3 (Part B): tropospheric degradation of aromatic volatile organic compounds, Atmos. Chem. Phys., 3, 181–193, doi:10.5194/acp-3-181-2003, 2003.

Kolb, C. E., Cox, R. A., Abbatt, J. P. D., Ammann, M., Davis, E. J., Donaldson, D. J., Garrett, B. C., George, C., Griffiths, P. T., Hanson, D. R., Kulmala, M., McFiggans, G., Pöschl, U., Riipinen, I., Rossi, M. J., Rudich, Y., Wagner, P. E., Winkler, P. M., Worsnop, D. R., and O' Dowd, C. D.: An overview of current issues in the uptake of atmospheric trace gases by aerosols and clouds, Atmos. Chem. Phys., 10, 10561–10605, doi:10.5194/acp-10-10561-2010, 2010.

cc BY

Kreidenweis, S. M. and Seinfeld, J. H.: Nucleation of sulfuric acid water and methanesulfonic acid-water solution particles: Implications for the atmospheric chemistry of organosulfur species, Atmos. Environ., 22, 283–296, 1988.

Kroll, J. H., Shailesh, R. S., Anderson, J. G., Demerjian, K. L., and Donahue, N. M.: Mechanism of HOx formation in the gas-phase ozone-alkene reaction, 2. Prompt versus thermal dissociation of carbonyl oxides to form OH, J. Phys. Chem. A, 105, 4446–4457, 2001.

Krouse, H. R. and Grinenko, V. A. (Eds.): Stable Isotopes: Natural and Anthropogenic Sulphur in the Environment, Scientific Committee on Problems of the Environment (SCOPE), vol. 43, J. Wiley & Sons, Chichester, 1991.

Larin, I. K., Messineva, N. A., Spasskii, A. I., Trofimova, E. M., and Turkin, L. E.: Measurement of the rate constants for the reactions of the $IO^•$ radical with sulfur-containing compounds H_2S, $(CH_3)_2S$, and SO_2, J. Kinetics and Catalysis, 41, 437–443, 2000.

Lin, X. and Chameides, W. L.: CCN formation from DMS oxidation without SO_2 acting as an intermediate, Geophys. Res. Lett., 20, 579–582, 1993.

Mauldin III, R. L., Berndt, T., Sipilä, M., Paasonen, P., Petäjä, T., Kim, S., Kurtén, T., Stratmann, F., Kerminen, V.-M., and Kulmala, M.: A new atmospherically relevant oxidant of sulphur dioxide, Nature, 488, 193–196 and supplement, 2012.

Mauldin III, R., Frost, G., Chen, G., Tanner, D., Prevot, A., Davis, D., and Eisele, F.: OH measurements during the First Aerosol Characterization Experiment (ACE 1): Observations and model comparisons, J. Geophys. Res., 103, 16713–16729, 1998.

Montgomery Jr., J. A., Frisch, M. J., Ochterski, J. W., and Petersson, G. A.: A complete basis set model chemistry. VI I. Use of the minimum population localization method, J. Chem. Phys., 112, 6532–6542, 2000.

O'Dowd, C. D., Jimenez, J. L., Bahreini, R., Flagan, R. C., Seinfeld, J. H., Hämeri, K., Pirjola, L., Kulmala, M., Jennings, S. G., and Hoffmann, T.: Marine particle formation from biogenic iodine emissions, Nature, 417, 632–636, 2002.

Ovadnevaite, J., Ceburnis, D., Leinert, S., Dall'Osto, M., Canagaratna, M., O'Brien, P., O'Doherty, S., Berresheim, H., and O'Dowd, C.: Distinct seasonal changes in marine aerosol composition and its properties, J. Geophys. Res., submitted, 2013.

Saiz-Lopez, A., Shillito, J. A., Coe, H., and Plane, J. M. C.: Measurements and modelling of I_2, IO, OIO, BrO and NO_3 in the mid-latitude marine boundary layer, Atmos. Chem. Phys., 6, 1513–1528, doi:10.5194/acp-6-1513-2006, 2006.

cc BY

Saiz-Lopez, A. and Plane, J. M. C.: Novel iodine chemistry in the marine boundary layer, Geophys. Res. Lett., 31, L04112, doi:10.1029/2003GL019215, 2004.

Saiz-Lopez, A., Plane, J. M. C., and Shillito, J. A.: Bromine oxide in the mid-latitude marine boundary layer, Geophys. Res. Lett., 31, L03111, doi:10.1029/2003GL018956, 2004.

Saunders, S. M., Jenkin, M. E., Derwent, R. G., and Pilling, M. J.: Protocol for the development of the Master Chemical Mechanism, MCM v3 (Part A): tropospheric degradation of non-aromatic volatile organic compounds, Atmos. Chem. Phys., 3, 161–180, doi:10.5194/acp-3-161-2003, 2003.

Schweitzer, F., Magi, L., Mirabel, P., and George, C.: Uptake rate measurements of methanesulfonic acid and glyoxal by aqueous droplets, J. Phys. Chem. A, 102, 593–600, 1998.

Seinfeld, J. H. and Pandis, S. N.: Atmospheres Chemistry Physics – From Air Pollution to Climate Change, chapters 8 and 11, J. Wiley & Sons, New York, 1360 pp., 1998.

Stone, D., Whalley, L. K., and Heard, D. E.: Tropospheric OH and HO_2 radicals: field measurements and model comparisons, Chem. Soc. Rev., 41, 6348–6404, 2012.

Stone, D., Blitz, M., Daubney, L., Howesa, N. U. M., and Seakins, P.: Kinetics of CH_2OO reactions with SO_2, NO_2, NO, H_2O and CH_3CHO as a function of pressure, Phys. Chem. Chem. Phys., 16, 1139–1149, 2014.

Taatjes, C. A., Welz, O., Eskola, A. J., Savee, J. D., Scheer, A. M., Shallcross, D. E., Rotavera, B., Lee, E. P. F., Dyke, J. M., Mok, D. K. W., Osborn, D. L., and Percival, C. J.: Direct measurements of conformer-dependent reactivity of the Criegee intermediate CH_3CHOO, Science, 340, 177–180, doi:10.1126/science.1234689, 2013a.

Taatjes, C. A., Shallcross, D. E., and Percival, C. J.: Research frontiers in the chemistry of Criegee intermediates and tropospheric ozonolysis, Phys. Chem. Chem. Phys., doi:10.1039/c3cp52842a, 2013b.

Tanner, D. J. and Eisele, F. L.: Present OH measurement limits and associated uncertainties, J. Geophys. Res., 100, 2883–2892, 1995.

Vereecken, L., Harder, H., and Novelli, A.: The reaction of Criegee intermediates with NO, RO_2, and SO_2, and their fate in the atmosphere, Phys. Chem. Chem. Phys., 14, 14682–14695, 2012.

Welz, O., Savee, J. D., Osborn, D. L., Vasu, S. S., Percival, C., Shallcross, D. E., and Taatjes, C. A.: Direct kinetic measurements of Criegee intermediate (CH_2OO) formed by reaction of CH_2I with O_2, Science, 335, 204–207, 2012.

cc BY

Table 1. Molecular parameters and energies for transition state theory calculations (see text for theoretical methods).

Species	Rotational constants GHz	Vibrational frequencies cm^{-1}	Relative energy[a] $kJ\,mol^{-1}$
ClO	18.03	829	–
SO_2	58.67, 10.17, 8.667	508, 1146, 1334	–
$ClO\text{-}SO_2^{\#}$	8.227, 1.831, 1.540	$248i$, 73, 135, 270, 296, 492, 720, 1113, 1303	24.1
BrO	12.50	713	–
$BrO\text{-}SO_2^{\#}$	8.138, 1.128, 1.011	$239i$, 63, 114, 227, 280, 494, 625, 1115, 1302	20.4
IO	9.844	649	–
$IO\text{-}SO_2^{\#}$	8.050, 0.8751, 0.8058	$258i$, 73, 109, 222, 292, 495, 613, 1107, 1288	7.3
OIO	18.31, 7.054, 5.092	273, 809, 831	–
$OIO\text{-}SO_2^{\#}$	4.572, 0.8714, 0.8385	$304i$, 29, 79, 129, 202, 261, 417, 495, 547, 810, 1064, 1247	50.1

[a] above the reactants, including zero-point energies

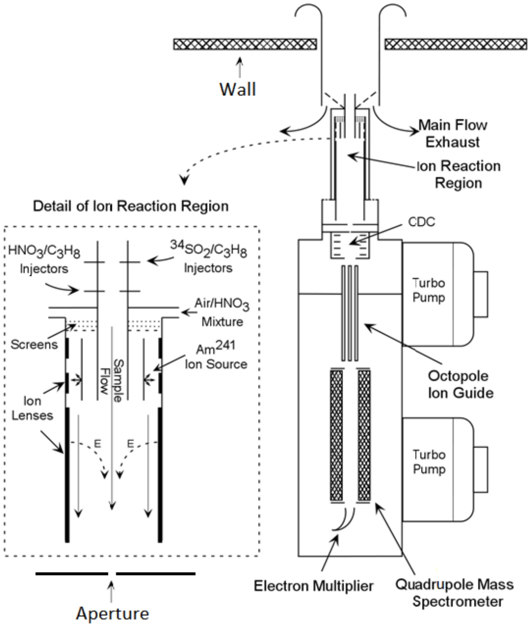

Fig. 1. Principle scheme of SI/CIMS components including air inlet (modified from R.L. Mauldin III, personal communication, 2012). Inset shows details of the atmospheric pressure region with reagent gas flows indicated for measurement of OH background signal (both $^{34}SO_2$ and C_3H_8 are added to the sample air through the two front injectors; see text). Laminar flow conditions with a central flow axis velocity of $0.71\,m\,s^{-1}$ in both the sample and ionization tubes are generated by a 12 slpm sample flow, 58 slpm total flow (= sample flow plus sheath flow, the latter indicated here by addition of Air/HNO_3 mixture), and the geometries of the sample tube (diameter 1.9 cm) and ionization tube (diameter 4.2 cm). The time needed (in each case starting at the first injector) to reach the second injector is 73 ms, to the entrance of the ionization region 115 ms, and to the aperture in front of the mass spectrometer 450 ms, respectively.

CC BY

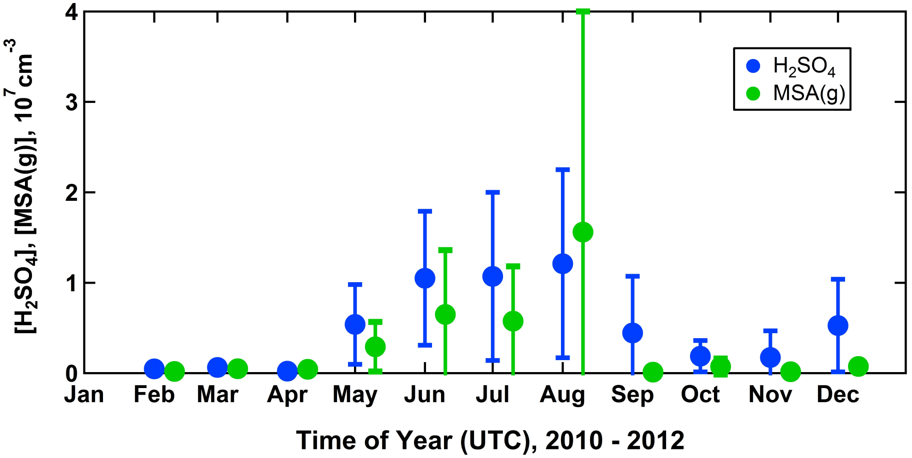

Fig. 2. Midday (10–14 h UTC) maximum H_2SO_4 and MSA(g) concentrations in marine air at Mace Head, averaged for each month (total measurement period: May 2010–August 2012).

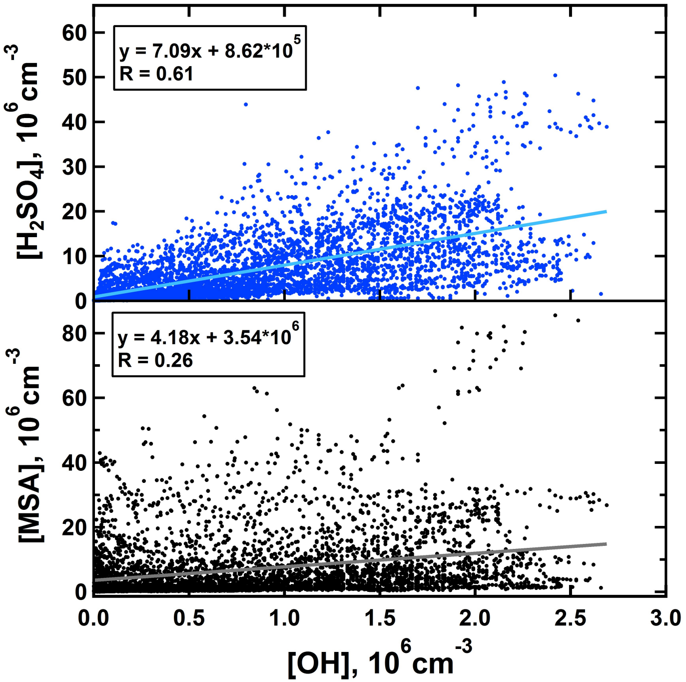

Fig. 3. Correlation between H_2SO_4 and OH (top) and between MSA(g) and OH concentrations (bottom) in marine air for the period May–August 2011 (5 min integrated data, daytime: 08:00–20:00 UTC). OH concentrations were calculated for the corresponding measurement times based on concurrent $J(O^1D)$ data and the $J(O^1D)$-OH relationship for marine air previously established in Berresheim et al. (2013).

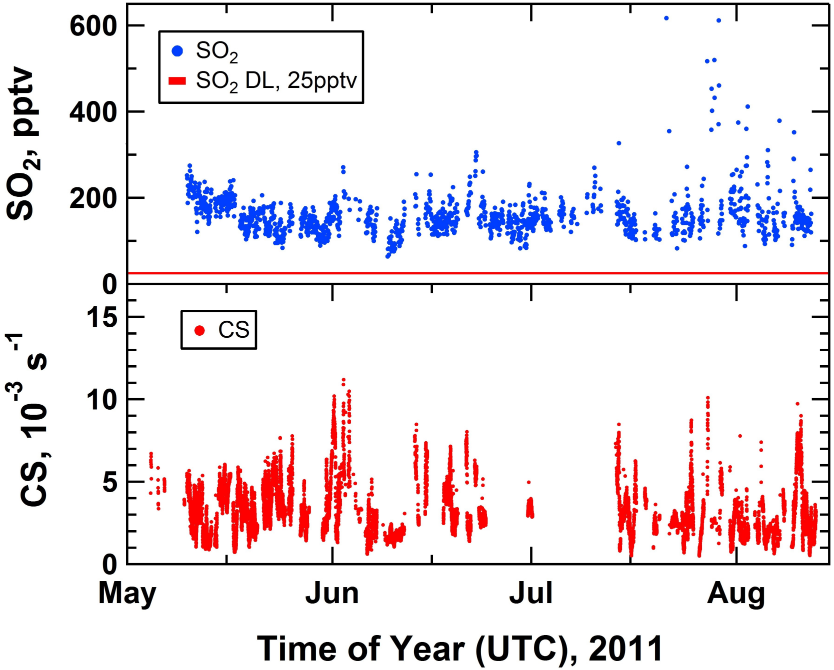

Fig. 4. (top) SO_2 mixing ratios (1 h signal integration) measured in marine air between May–August 2011 (average: 169 (±50) pptv; detection limit: 25 pptv, indicated by red line); (bottom) Condensational sink (CS; 5 min integration) calculated for H_2SO_4 (see text).

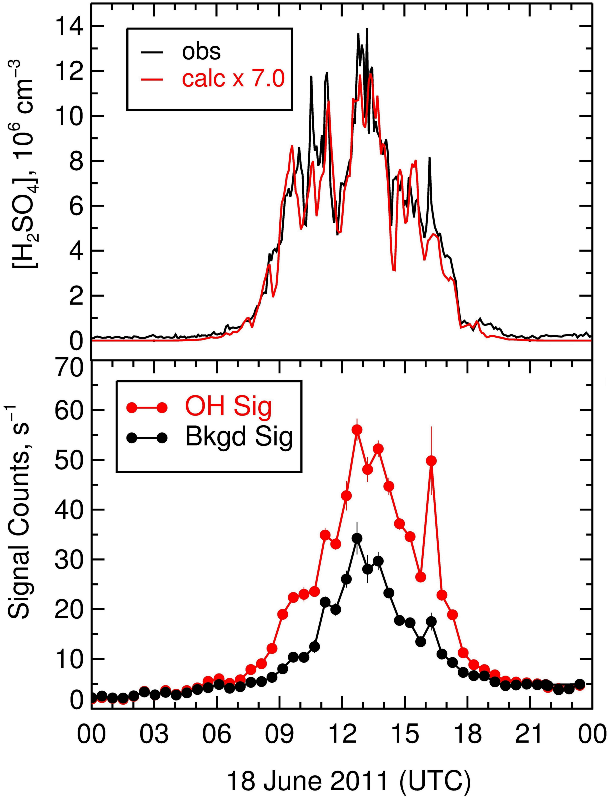

Fig. 5. Example of observed ambient H_2SO_4 concentration in comparison with H_2SO_4 mass balance values calculated from Eq. (1) for 18 June 2011. The OH concentrations used for the calculations were derived from the OH-$J(O^1D)$ relation established for the marine sector (Berresheim et al., 2013) (continuous 5 min time resolution). (top) Mean discrepancy factor of 7.0 between midday (10–14 UTC) observed and calculated $[H_2SO_4]$. (bottom) Signal counts obtained for OH measurement and OH background mode (cycle: 5 min during each 30 min period).

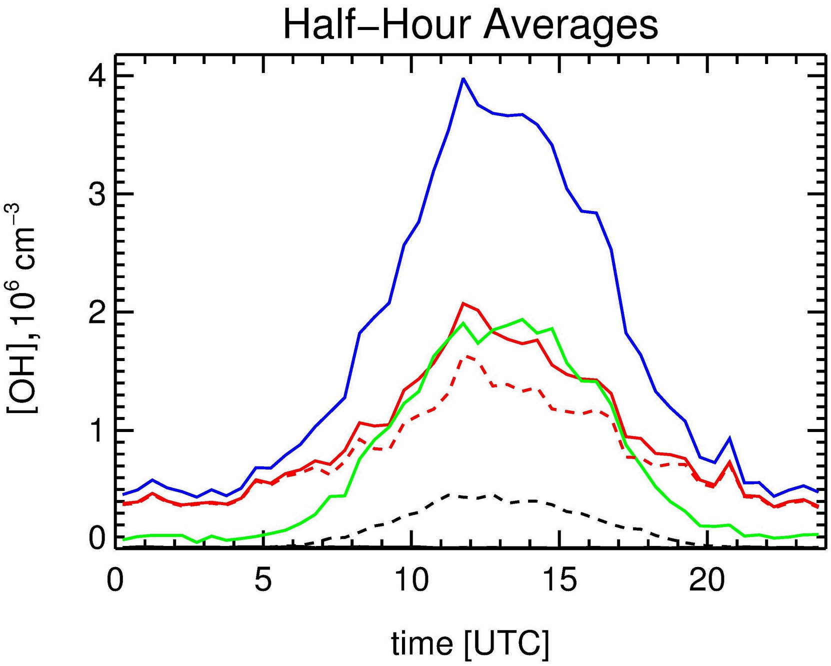

Fig. 6. Mean half-hour values measured in marine air of the OH mode raw signal at m/z 99 (blue line), total background mode raw signal at m/z 99 (red line), OH mode signal minus background mode signal (green line = net signal counts corresponding to the ambient OH concentration), signal counts at m/z 99 due to ^{34}S mass fraction of ambient H_2SO_4 (black dashed line = signal(m/z 97) $\cdot$ 0.044), OH mode background signal with ^{34}S fraction of ambient H_2SO_4 subtracted (red dashed line).

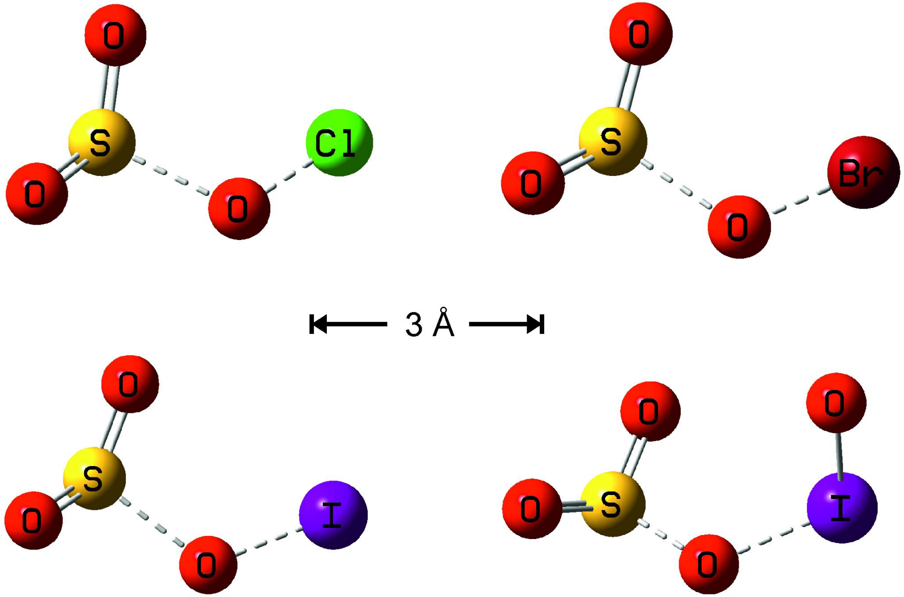

Fig. 7. Transition state geometries for ClO, BrO, IO and OIO + SO_2.

cc BY

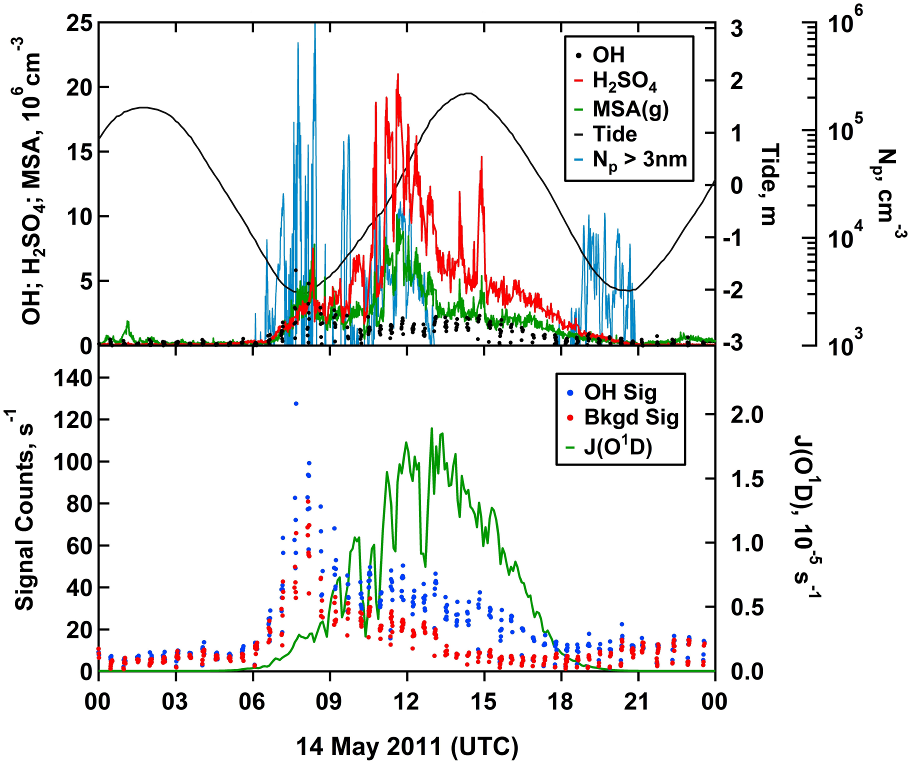

Fig. 8. Example of increased OH background signal during two aerosol nucleation events at low tide under marine sector conditions (07:00–09:00 UTC; 18:30–21:00 UTC). (top) OH, H_2SO_4 and MSA(g) concentrations (30 s integration), tidal height, and total particle number concentration $N_p > 3$ nm diameter (30 s integration) measured with a condensation particle counter (CPC; TSI 3025). (bottom) Count rates for OH and (non-OH) background signals (30 s) and ozone photolysis frequency, $J(O^1D)$.

CC BY